Mutations of Arginine 64 within the Putative Ca^{2+}-Binding Lumenal Interhelical a−b Loop of the Photosystem II D1 Protein Disrupt Binding of the Manganese Stabilizing Protein and Cytochrome c_{550} in *Synechocystis* sp. PCC6803[†]

Zhao-Liang Li and Robert L. Burnap*

Department of Microbiology and Molecular Genetics, Oklahoma State University, Stillwater, Oklahoma 74078

Received January 3, 2001; Revised Manuscript Received June 26, 2001

ABSTRACT: Mutations D1-R64E, D1-R64Q, and D1-R64V in the putative calcium-binding lumenal interhelical a−b loop of the photosystem II (PSII) D1 protein were characterized in terms of impact on growth, extrinsic protein binding, photoactivation, and properties of the H_2O-oxidation complex. The D1-R64E charge reversal mutation greatly weakened the binding of the extrinsic manganese-stabilizing protein (MSP) and, to a considerably lesser extent, weakened the binding of cytochrome c_{550} (c550). Both D1-R64Q and D1-R64E exhibited an increased requirement for Ca^{2+} in the cell growth medium. Bare platinum electrode measurements of O_2-evolving membranes showed a retarded appearance of O_2 following single turn-over flashes, especially in the case of the D1-R64E mutant. The D1-R64E mutant also had a pronounced tendency to lose O_2 evolution activity in the dark and exhibited an increased relative quantum yield of photoactivation, which are characteristics shared by mutants that lack extrinsic proteins. S_2 and S_3 decay measurements in the isolated membranes indicate that D1-R64E and D1-R64Q have faster decays of these higher S-states as compared to the wild-type. However, fluorescence decay in the presence of DCMU, which monitors primarily Q_A^- charge recombination with PSII donors, showed somewhat slower decays. Taken together, the fluorescence and S-state decay indicate that the midpoint of either Q_B^- has been modified to be more negative in the mutants or that a recombination path presumably involving either Q_B^- or Y_D has become kinetically more accessible.

The photosystem II (PSII)[1] reaction center complex catalyzes the light-driven reduction of plastoquinone using electrons extracted from water via the oxygen-yielding H_2O-oxidation reaction (for reviews on PSII see refs *2*−*5*). Light-driven charge separation results in the reduction of plastoquinone on the acceptor side of the photochemical reaction center and the oxidation of P680, a dimeric chlorophyll species, on the donor side of the PSII complex. $P680^+$ is a strong oxidant capable of oxidizing water, and Y_z is the redox active tyrosine 161 of the reaction center D1 protein. The sequential oxidation of the H_2O-splitting enzyme causes it to cycle through a series of intermediate redox states termed S-states (S_i, where $i = 0-4$), corresponding, at least in part, to the stepwise oxidation of a Mn tetramer $(Mn)_4$ at the catalytic site by $P680^+$. The oxidation of Y_z by reaction center chlorophyll $P680^+$ results in the formation of the neutral radical $Y_z^\bullet$ with the release of a proton occurring concomitantly upon transfer of an electron to $P680^+$. The mechanism of H_2O-oxidation remains to be resolved; however, proton-coupled electron transfer or hydrogen atom abstraction involving $Y_z^\bullet$ are among proposals currently being considered (*3*, *4*, *6*−*9*).

Considerable progress toward determining the three-dimensional structure of PSII has been made (*1*, *10*−*15*). Most recently, the structure of an O_2-evolving PSII complex isolated from the thermophilic cyanobacterium, *Synechococcus elongatus*, was solved to a resolution as high as 3.8 Å (*1*) (Protein Data Bank entry 1FE1). This complex contains at least 17 subunits, of which 14 are intrinsic membrane proteins. While the current structural resolution does not permit modeling of the amino acid locations within the structure,[2] it has led to assignments of the major reaction center core polypeptides with respect to their transmembrane helices. Helix assignments are made for the "photochemical core" PSII complex, which contains at least six major membrane-spanning protein subunits: D1, D2, CP43, CP47, the *psbI* gene product, and the α and *β* subunits of cytochrome b_{559}. These highly conserved intrinsic proteins bind the pigments and cofactors involved in light-induced charge separation and electron transport and are found in

[†] This work was funded by the National Science Foundation (MCB 9728754).

* Corresponding author: Robert L. Burnap. Phone: 405-744-7445. Fax: 405-744-6790. E-mail: burnap@biochem.okstate.edu.

[1] Abbreviations: Chl, chlorophyll; Cyt. c_{550}, cytochrome c_{550} encoded by the *psbV* gene; DCBQ, 2,6-dichloro-*p*-benzoquinone; DCMU, 3-(3,4-dichlorophenyl)-1,1-dimethylurea, inhibits electron transport between Q_A and Q_B; HA, hydroxylamine (NH_2OH); a−b loop, lumenally exposed interhelical loop situated between transmembrane helices a and b of the D1 reaction center protein; Hepes, 4-(2-hydroxyethyl)-1-piperazineethanesulfonic acid; $(Mn)_4$, tetranuclear Mn cluster functioning in H_2O-oxidation; MSP, manganese-stabilizing protein, extrinsic 33 kDa PSII protein; *psbA*, gene encoding the reaction center D1 protein; *psbO*, gene encoding the manganese-stabilizing protein; TMBZ, (3,3′,5,5′-tetramethylbenzidine); Y_Z, redox active tyrosine of the D1 protein acting as secondary electron donor of the reaction center.

[2] Specific electron densities have been attributed to the redox active tyrosines, Y_Z and Y_D, of the D1 and D2 proteins, respectively (*1*). However, these are the exception in the current published structure.

10.1021/bi0100135 CCC: $20.00
Published on Web 07/28/2001

all organisms capable of oxygenic photosynthesis. An electron-dense region located in the lumenal portion of the D1 protein has been ascribed to the $(Mn)_4$ in accordance with numerous biochemical and site-directed mutagenesis experiments indicating D1 provides ligands to the active site metal cluster (for review, see ref *5*). However, the locations for Ca^{2+} and Cl^- ions, essential cofactors of the H_2O-oxidation reaction, remain unresolved.

In addition to the intrinsic polypeptides, extrinsic PSII subunits, associated with the H_2O-oxidation domain, are found in all PSII-containing taxa. The extrinsic polypeptides stabilize the $(Mn)_4$, modulate the binding of Ca^{2+} and Cl^- ions, and optimize the catalytic efficiency of the H_2O-oxidation reaction (see refs *2*, *5*, and *16*). Among the extrinsic proteins associated with the WOC, the manganese-stabilizing protein (MSP), encoded by the *psbO* gene, is associated with all taxonomic variants of PSII. However, the remaining complement of extrinsic proteins associated with the WOC exhibit what is essentially a dichotomous phyletic distribution. On one hand, the WOC of all green plants and green algae contains the 23- and 18-kDa proteins, which are encoded by the *psbP* and *psbQ*, respectively. In contrast to higher plants and green algae, the WOC in all other PSII-containing organisms contains a c-type cytochrome, cytochrome c_{550} (*psbV* gene product) and a 9−12 kDa protein (*psbU* gene product), in addition to MSP. The function of cytochrome c_{550} remains unresolved. However, it has an unusually low midpoint potential estimated to be −250 mV that is partly attributable to a bis-histidyl axial ligation of the heme iron (*17*). Recently, the crystal structure of isolated cytochrome c_{550} from the cyanobacterium *Synechocystis* sp. PCC6803 has been solved to 1.26 Å resolution (*18*). An additional subunit, with an estimated mass of 20 kDa, is associated with the WOC of the thermophilic red alga, *Cyanidium caldarium*, and appears to be involved in the stabilization of the binding of the other three extrinsic polypeptides of the WOC (*19*).

The extrinsic proteins, together with interhelical loops connecting the transmembrane portions of the complex, form the large protein mass that extends approximately 55 Å into the aqueous phase of the thylakoid lumen and contains the H_2O-oxidation domain of the complex (*1*). In the *Synechococcus* PSII crystal structure, this mass remains largely unresolved. However, approximately half of MSP and the majority of cytochrome c_{550} are identified within this mass. The contact sites of MSP and cytochrome c_{550} with the intrinsic subunits remain unresolved in the crystal structure, but biochemical and genetic evidence has provided some information in this regard (reviewed in refs *2*, *5*, and *16*). Several lines of evidence point to direct interaction between the lumenally exposed e-loop of CP47 and MSP, although contacts with additional intrinsic subunits are likely. Chemical cross-linking and modification experiments have mapped probable contact sites between specific domains of MSP and the CP47 e-loop (*20*−*23*), whereas deletion mutagenesis has defined sets of residues in the same region as important for the binding interaction (*24*). Mutations of the pair of arginine residues at positions 384 and 385 on the e-loop (R384R385) were found to disrupt the binding of MSP to the reaction center (*21*). These results are consistent with data indicating that positively charged residues on the intrinsic portion of the PSII complex and negatively charged residues on MSP as contributing to the ion-pair stabilization of MSP binding (*16*, *26*). This assessment is in line with the results of Isoagi et al. indicating binding depends on a positively charged surface of the intrinsic proteins (*27*). On the other hand, these results have been questioned, and the involvement of positively charged residues on MSP interacting with acidic groups on the intrinsic subunits has been posited (*23*). Less information is available on the binding sites of the other extrinsic proteins. The binding of the 23-kDa protein to the reaction center reportedly depends on the presence of bound MSP according to several studies (*28*−*30*); however, release of MSP is reported to occur without the concomitant release of the 23-kDa protein (*31*), and mutants unable to synthesize MSP still bound the 23-kDa protein to the membranes (*32*). Similarly, the binding of cyanobacterial cytochrome c_{550} was reported to be partially dependent upon bound MSP (*33*) and has been found to chemically cross-link with D2, MSP, and the 12-kDa protein in situ (*34*). On the other hand, binding of cytochrome c_{550} was found to be independent of MSP binding in the red alga *C. caldarium* (*19*) and has functions independent of MSP (*35*).

In this report, we describe the effects of substitution mutations at the highly conserved arginine residue, R64, in the a−b loop of the D1 protein. The a−b loop of the D1 protein is hypothesized to participate in the binding of PSII Ca^{2+} and is situated in a region that may be involved in the binding of MSP according to the crystal structure (*1*). Previous analysis of mutations of strictly conserved acidic groups revealed slow downs of the S-state transitions (*36*, *37*) that are attributable to alterations on the donor side of Y_Z (*36*) as well as a destabilization of the intermediates in the light-driven assembly of the $(Mn)_4$ (*37*). Here we find that mutations of the adjacent R64 residue impair the binding of the extrinsic proteins, especially MSP, increase the requirement for Ca^{2+} during cell growth, and alter the redox properties of the H_2O-oxidation complex.

MATERIALS AND METHODS

Construction and Growth of Strains. The naturally transformable, glucose-utilizing strain of *Synechocystis* sp. PCC6803 (*38*) was used in the construction of all of the strains described here. For routine manipulations, the wild-type and mutant cyanobacterial strains were grown on a rotary shaker in BG-11 media supplemented with 5 mM glucose. To determine the autotrophic growth under calcium-limiting conditions, 0.24 mM $CaCl_2$ in the normal BG-11 medium was replaced by 0.48 mM NaCl. Construction and characterization of the D1-R64E, D1-R64Q, and D1-R64V strains were performed as previously described (*37*, *39*) using the *psbA2*-containing plasmid pRD1031 and the triple *psbA* deletion strain 4E-3, both generous gifts from Prof. R. Debus, University of California Riverside. The strain of 4E-3 transformed by the psbA-containing plasmid pRD1031 was used as a control and designated wild-type here (*39*).

Isolation of O_2-Evolving Membranes and Extrinsic Protein Binding Assays. Isolation of O_2-evolving membranes was performed with modifications of previously described procedures (*40*, *41*). Cells from 100 mL of late logarithmic phase cultures were harvested by centrifugation at 6000 rpm for 10 min at 4 °C in a Sorvall GSA rotor. Following harvest, cells were resuspended in approximately 1.2 mL of HMCS

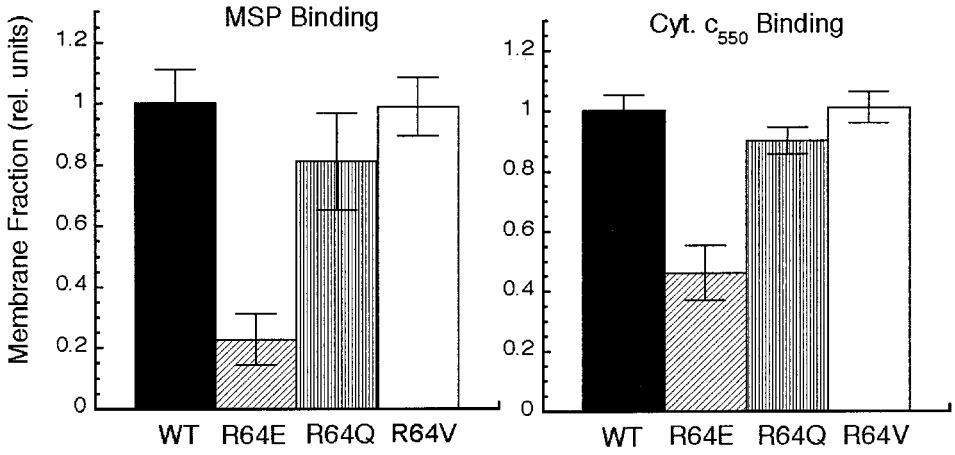

FIGURE 1: Quantification of the amounts of MSP (panel A) and cytochrome c_{550} (panel B) bound to isolated thylakoid membranes in wild-type control and D1-R64 site-directed mutants. Histograms represent the results of densitometic analysis of electrophoretically separated proteins in isolated and washed membrane samples. Washed membranes were subjected to gel electrophoresis and immunoblot analysis of the manganese-stablizing protein (MSP) and in situ heme-stain analysis of cytochrome c_{550}. SDS−PAGE was performed with 12% polyacrylamide separation gel and 6 M urea; cytochromes were detected by TMBZ (*40*). Immunoblot analysis of MSP involved transfer of separated proteins to PVDF membrane reaction with polyclonal anti-MSP antibodies and detection of the antigen−antibody complex using horseradish peroxidase-conjugated goat anti-rabbit IgG (Bio-Rad). The error bars represent standard deviations of three experiments.

buffer (50 mM Hepes, 5 mM $CaCl_2$, 10 $MgCl_2$, 1 M sucrose, pH 7.2) and supplemented with 1 mM each of PSMF, ϵ-caproic acid, and benzamidine to inhibit protease activity and incubated on ice for 1 h. Cells were mechanically broken by shaking 1 mL of the cell suspension with 0.6 volumes of 0.1 mm glass beads using a Mini-Bead Beater machine (Bio-Spec Products, Bartlesville, OK, USA). After breakage, the glass beads, unbroken cells, and debris were pelleted from the cell lysate by centrifugation in a microcentrifuge at 3000 rpm for 3 min at 4 °C. The membranes from the resultant supernatant were collected by centrifugation at 70 000 rpm for 30 min at 4 °C in a Beckman TLA 100.3 rotor and resuspended in 200 μL of HMCS buffer. The membranes were used immediately or were aliquoted and stored at −80 °C.

Assay for the binding of extrinsic proteins was performed with freshly broken cells using previously described procedures (*42*, *43*). Cells were homogenized as above, and the resultant lysates were adjusted to 400 μg of chlorophyll·mL^{-1} and treated with the nonionic detergent β-dodecyl maltoside (Anatrace, Maumee, OH) at a final concentration of 0.03% to minimize the entrapment of unbound extrinsic polypeptides in membrane vesicles. After incubation on ice for 10 min, the membranes were collected by centrifugation at 70 000 rpm for 30 min at 4 °C in a Beckman TLA 100.3 rotor, the pellets were washed again with HMCS buffer containing of 0.03% β-dodecyl maltoside, and the washed membranes were resuspended in HMCS buffer at 400 μg of chlorophyll·mL^{-1}. SDS−PAGE was performed on a 12% polyacrylamide separation gel containing 6 M urea. Immunoblot analysis was performed as described earlier (*40*), except electrophoretically separated samples were immobilized on PVDF membranes (Bio-Rad, Richmond, CA). Cytochrome c_{550} was detected on the basis of its heme-centered peroxidase activity using the chromogenic substrate TMBZ (3,3′,5,5′-tetramethylbenzidine) as described by Shen et al. (*44*). Relative quantities of the amounts of extrinsic proteins were estimated by densitometry of the corresponding immunoblots and heme-stained gels using an image acquisition and analysis system (AlphaImager/TotalLab, Alpha Innotec Corp., San Leandro, CA).

Fluorescence Measurements. Measurements of variable fluorescence yields were performed using a Walz PAM 101 chlorophyll fluorometer equipped with PAM 103 flash attachment (Walz Inc. Germany). Cells in late logarithmic phase of growth were harvested by centrifugation. After being washed with HN buffer (10 mM Hepes, pH 7.0, 30 mM NaCl), the cells were resuspended in HN buffer at a final concentration of 50 μg of Chl·mL^{-1} and maintained under dim light (less than 1 h) on the shaker at 150 rpm before being used for experiments. Estimation of the concentration of charge-separating PSII centers was performed essentially as described previously (*41*−*43*).

O_2 Evolution Measurements and Photoactivation. O_2 evolution measurements using a Clark-type electrode and a bare platinum electrode to measure steady-state and flash yield activities were performed as described previously (*37*). Hydroxylamine (HA) extraction of PSII Mn in whole cells and photoactivation of the resultant samples were performed according to Cheniae and Martin (*48*) with modifications as described previously extracted samples (*43*, *49*).

Chlorophyll Determination. The chlorophyll a concentration in this paper was measured in methanol extracts according to Lichtenthaler (*50*) using the extinction coefficient at 665.2 nm of 79.24 mg^{-1} cm^{-1}.

RESULTS

Figure 1 depicts binding assays for cytochrome c_{550} and MSP to membranes using previously established methods (*42*, *43*). In these experiments, total cell lysates from mutant and control cells were centrifugally separated into membrane and soluble fractions and analyzed for MSP and c-type cytochrome content. Isolation and washing of the membranes was done in the presence of low concentrations of the nonionic detergent dodecyl maltoside to promote the release of unbound proteins from membrane vesicles. As shown in Figure 1, the amounts of MSP and cytochrome c_{550} retained on the washed thylakoid membranes were estimated by

Table 1: Photosynthetic Characteristics of D1-R64 Site-Directed Mutants of Synechocystis sp. PCC6803

stains	rate of oxygen evolution[a]	variable fluores yield [b]	autotrophic growth: normal BG-11 medium	autotrophic growth: Ca^{2+}-limiting BG−11 medium
wild-type*	100	100	+	+
R64E	35	44	+	−
R64Q	76	71	+	−
R64V	97	97	+	+

[a] Normalized to control rate of 679 μmol of O_2 (mg of Chl) $^{-1}$ h^{-1}. Oxygen evolution was measured at a chlorophyll concentration of 6.25 μg/mL in HN buffer (10 mM Hepes, 30 mM NaCl, pH 7.2) with the addition of 750 μM DCBQ and 2 mM $K_3Fe(CN)_6$. The data were an average of three or more independent measurements. [b] Normalized to a variable fluorescence yield of 0.47 for the control. Measurements were taken in the presence of 20 mM hydroxylamine and 40 μM DCMU essentially as in refs *46* and *47*. The data were an average of three independent measurements. A PAM 101 chlorophyll fluorometer with a PAM 103 triggering attachment (Walz Inc. Germany) was used in this experiment.

densitometry of immunoblots and heme-stained gels, respectively (see Materials and Methods). As shown in Figure 1, the amount of MSP bound to D1-R64E thylakoids decreased to approximately 20% relative to the wild-type, whereas the D1-R64Q and D1-R64V mutants showed little or no significant decrease in the association of MSP with the membrane fraction. The amount of cytochrome c_{550} retained by washed D1-R64E membranes was also decreased but not as dramatically (approximately 40% retained in the membrane fraction) as observed for MSP.

Table 1 shows the relative concentration of PSII centers in mutant and control cells estimated by variable fluorescence (*51*) as well as the maximal rates of O_2 evolution using the artificial electron acceptor DCBQ. Maximal rates of steady-state O_2 evolution approximately paralleled the estimated concentration of PSII. The parallel relationship is close except for D1-R64E, which displays a disproportionately lower rate of O_2 evolution than the estimated concentration of PSII (35 vs 44%). This may be due to the presence of a fraction of PSII centers capable of charge separation but incapable of O_2 evolution. Alternatively, the D1-R64E mutation results in a slowed enzymatic turnover of PSII and a consequent slowing of the light-saturated rate of O_2 evolution. A slowed turnover rate is consistent with bare platinum electrode measurements (see below) that indicate that the O_2 release kinetics are retarded in this mutant.

The autotrophic growth characteristics of the R64 mutants in the presence and absence of added Ca^{2+} in the cell growth medium were examined. Previous studies have shown that certain mutations prevent growth in the absence of added Ca^{2+}, whereas the wild-type is capable of growth without added Ca^{2+} relying on the relatively low background levels present in the media prepared under standard conditions. As with the proximally located mutations of D1-D59 and D1-D61 in the a−b loop of the D1 protein (*46*), both the D1-R64E and D1-R64Q mutations abolish the ability of cells to grow in the Ca^{2+}-limiting BG-11 medium (Table 1).

Patterns of flash O_2 yields of isolated membranes centrifugally deposited on a bare platinum electrode provide information of the S-state cycling kinetics of the WOC and are shown in Figure 2A. The amplitudes of the O_2 signals of the mutants are lower than the wild type consistent with

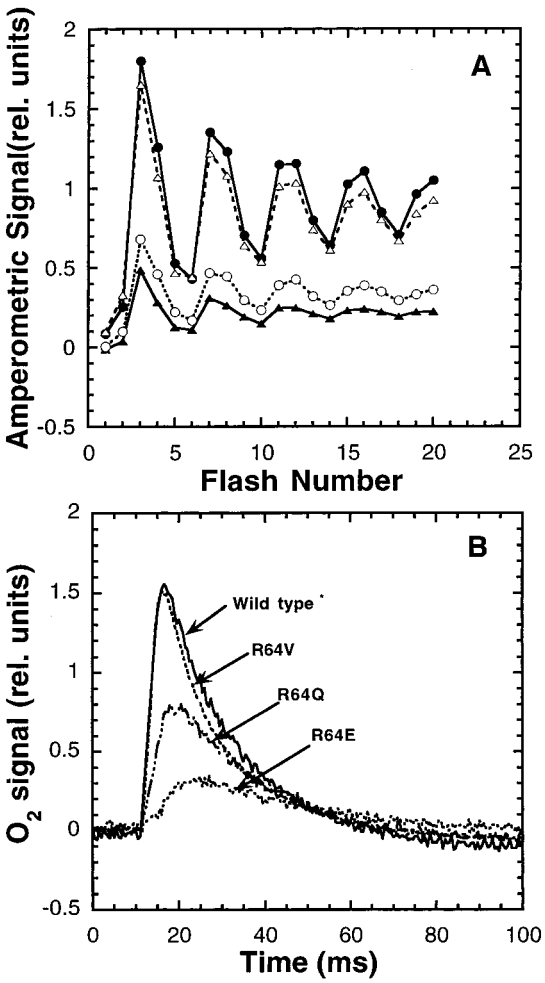

FIGURE 2: Flash O_2 yields of isolated membranes. Oxygen production by dark-adapted wild-type and mutant membranes that have been centrifugally deposited upon the surface of a bare-platinum electrode and given a sequence (4 Hz) of saturating xenon flashes. Panel A shows a oscillatory pattern of O_2 production as a function of flash number by control, closed circles; R64Q, open circles; R64E, closed triangles; and R64V, open triangles. Panel B: Oxygen signals of mutant and wild-type membranes. The exponential rise times of the depicted signals are given in Table 2. Kinetic analysis of the data was performed according to the exponential method described in Jursinic and Dennenberg, 1990. After deposition on the electrode surface, membranes were given a sequenced of 20 pre-flashes, dark adapted for 10 min, and then the measuring flashes were applied.

the lower concentration of PSII centers and lower maximal rates of O_2 evolution present in these samples. However, the amplitude of the O_2 signals of D1-R64Q membranes is disproportionately lower than the whole cell measurements of maximal steady-state activity would otherwise suggest (Table 1). The mutation therefore renders the O_2 evolution activity labile during the isolation of membranes. Additionally, the relatively large miss factor associated with S-state turnover in the D1-R64E and D1-R64Q mutants probably also contribute to the lowered per flash O_2 yields, as could the decreased stability of the S_2 and S_3 states (see below). However, analysis (not shown) of these contributions indicates that they would not fully account for the disparity and that lability of activity therefore appears to be the major cause for the difference. The loss does not, however, correlate with the loss of the extrinsic proteins since we observe little loss of either cytochrome c_{550} or MSP in the isolated D1-R64Q

Table 2: S-State Decay Cycling Parameters[a]

strain	10 min dark s-state distribution: $S_0/S_1/S_2/S_3$(%)	misses α, (%)	hits β, (%)	double hits γ, (%)	O_2 release[b], $t_{1/2}$, membranes (ms)
RD1031	34/60/4/2	7	90	3	1.3
R 64 E	31/64/5/0	12	85	3	6.1
R 64 Q	31/64/5/0	12	85	3	3.5
R 64 V	29/60/8/3	8	89	3	1.3

[a] Samples were given a series of 20 pre-flashes prior to the 10 min dark period preceding the series of measuring flashes. Numerical analysis of the amplitudes was performed using either 4- or 5-state models as described previously (*74*, *75*). The 4- and 5-state models produced essentially equivalent results and no evidence for the presence of an S_{-1} "super-reduced" state in any of the samples could be demonstrated using the 5-step models. [b] Oxygen release kinetics were estimated from the rising portion of the O_2 signal (Figure 2) using the exponential method as described previously (*76*).

membrane preparation (Figure 1). Thus, the lability of O_2 evolution may be due to improper or weak binding of the extrinsic proteins. The basis for this loss was not pursued further, although experiments with different buffers (e.g., containing higher $CaCl_2$ concentrations) did not reveal conditions restoring the activity. The oscillatory pattern of O_2 yields with maxima on the third flash and a period four oscillation thereafter in all samples indicates a fairly normal operation of the S-state cycling mechanism in the mutants. Numerical evaluation of the yield patterns presented in Table 2 show that the D1-R64E and D1-R64Q mutants result in an increase miss factor. The increased miss factor, which corresponds to a decreased probability that a given flash will be converted into a productive advancement of the H_2O-splitting enzyme, results in the more pronounced damping of the oscillatory pattern as the flash sequence progresses. The analysis does not, however, provide information as to which S-state transition(s) are affected by the increased miss probability. However, the decreased stability of the S-states in these mutants, particularly the S_2 state, (below) may contribute to the increased miss factor.

Kinetics of O_2 release during the S_3-[S_4}-S_0 transition are shown in Figure 2B and quantified in Table 2. It is observed that D1-R64Q and, especially, D1-R64E exhibit retarded kinetics of O_2 release. Since the D1-R64E mutant exhibits impaired binding of the extrinsic proteins and since the absence of MSP results in slow downs of O_2 release kinetics, the absence of MSP binding may be responsible for the retarded O_2 release observed in the D1-R64E mutant. On the other hand, the D1-R64Q mutant also exhibits a slowed O_2 release kinetic, and it does not appear to lose the extrinsic proteins during the isolation of membranes. Therefore, the slow downs observed for these mutations are probably not due to the loss of extrinsic proteins.

Figure 3 illustrates the results of measurements of the dark stability of the S_2 and S_3 states performed in isolated membranes. The lifetimes of the S_2 and S_3 states were estimated using double flash techniques (*25*, *37*, *47*). This involves flashing dark-adapted membrane samples to advance them to these more oxidized states of the H_2O-splitting enzyme. Then, after varying time intervals, measured for the extent of relaxation as judged by the amplitude of the O_2 yield on the third flash as a function of the time interval between the first and second or the second and third, flashes, for the S_2 and S_3 lifetimes, respectively. The dark decay of the S_2 and S_3 states corresponds to the rereduction of the H_2O-splitting enzyme by electrons from the acceptor side of the PSII complex, from the redox active tyrosine, termed Y_D, on the donor side of the complex, and ill-defined "endogenous donors" (e.g., see ref *52*). Accelerated S-states decays were observed in the D1-R64E mutant, and to a lesser extent in the D1-R64Q mutant, indicating that the mutations alter the redox properties of the recombining charge pairs in terms of their reactivity toward each other. Since other mutations in the a−b loop of D1 appear to modify the redox properties of the $(Mn)_4$ cluster and also exhibit accelerated S-state decays, it is possible that the accelerated S-state decays are due to a more positive redox potential of the $(Mn)_4$ cluster resulting in a larger redox difference between the donor and acceptor sides in these mutants (but see below).

If the accelerated S-states decays observed in the D1-R64E mutant are due to changes in the midpoint potential of the S_2 and S_3 states of the $(Mn)_4$ cluster, then the recombination of the $S_2Q_A^-$ state, observable by monitoring the decay of variable fluorescence following a flash, might also be expected to exhibit an accelerated rate of decay. Figure 4 depicts the fluorescence decays of the R64 mutants in the presence of DCMU. Clearly, an acceleration of S-state decay is not detected, but instead a deceleration of fluorescence

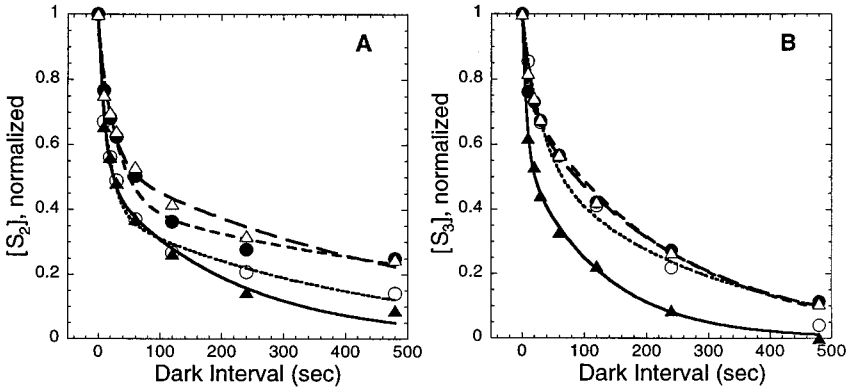

FIGURE 3: S-state decay. Decay of the S_2 state (panel A) and decay of the S_3 state (panel B) in membranes of the wild-type, closed circles; R64Q, open circles; R64E, close triangles; and R64V, open triangles. Measurements of the lifetimes of the S_2 state was performed by recording the amplitude of O_2 yield on the third flash under conditions varying the time interval between the first and second flashes. Measurement of the lifetime of the S_3 state in each of the different strains was performed by recording the amplitude of O_2 yield on the third flash under conditions varying the time interval between the second and third flashes (*47*, *77*, *78*).

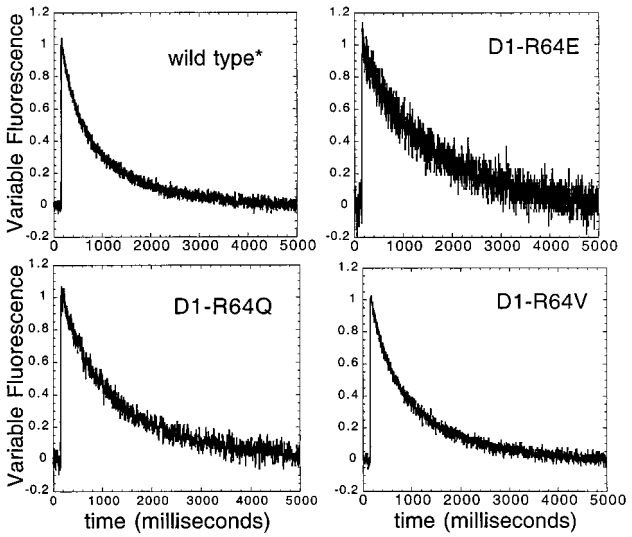

FIGURE 4: Fluorescence yield kinetics of Q_A^- reoxidation. The decays of Q_A^- in wild type and R64 mutant cells in the presence of DCMU, following a saturating single turnover xenon flash as measured by changes in the yield of chlorophyll a fluorescence using a PAM fluorometer with a PAM 103 triggering attachment (Walz Inc.). The cells were incubated in darkness for 5 min before measuring pulses were switched on at 1.6 kHz and the flash was given at 100 ms later in the presence of 20 μM of DCMU. Each trace represents the average of 10 recordings performed on the same sample.

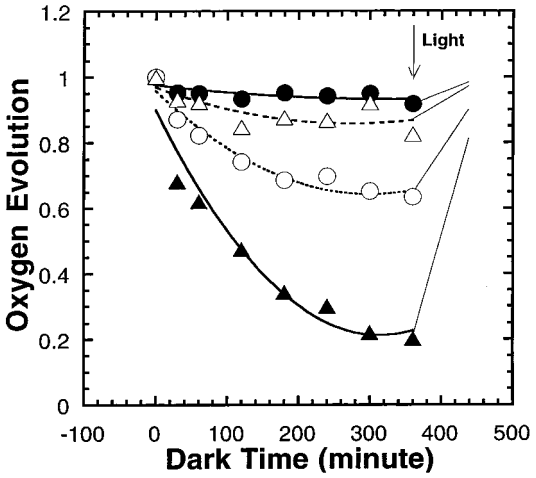

FIGURE 5: Dark stability of O_2-evolving activity. A Clark-type electrode was used to measure steady-state O_2 evolution. Cells of wild-type, closed circles; R64Q, open circles; R64E, closed triangles; and R64V, open triangles. were incubated on a rotary shaker (Gyrotory Shaker-Model G2, New Brunswick Scientific Co.) at 150 rpm in the dark, for recovery experiments, cells were transferred to the rotary shaker and incubated under growth light. Maximal rates of O_2 evolution were determined polarographically at 30 °C using a Clark-type electrode at a final chlorophyll concentration of 6.25 μg·mL^{-1}. Samples were resuspended in HN buffer supplemented with 0.75 mM DCBQ and 2 mM potassium ferricyanide.

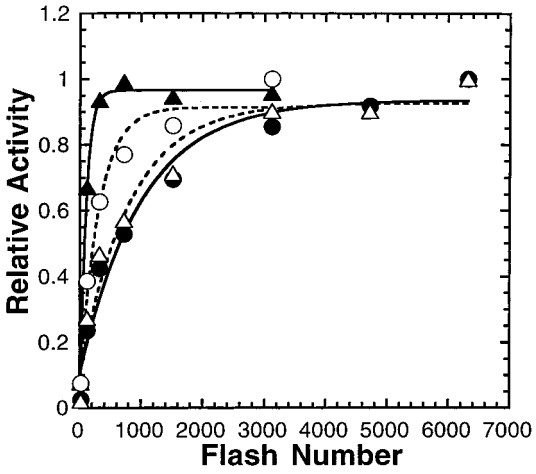

FIGURE 6: Photoactivation of hydroxylamine extracted samples as a function of flash number. Development of O_2 during a sequence of photoactivating flashes in Mn-extracted cells of the wild-type, closed circles; R64Q, open circles; R64E, closed triangles; and R64V, open triangles. The photoactivating light consisted of a sequence of saturating, single turn-over xenon flashes given at a fixed frequency of 4 Hz. Cells were centrifuged to the electrode surface and subjected to the photoactivating flash sequence given without electrode polarization. Data points represent the normalized amplitudes of the O_2 signal obtained as the average O_2 signal amplitude of the last four flashes of a 20 flash 4 Hz measuring flash sequence on the polarized electrode initiated 10 s following the photoactivating flash sequence. Data points represent the averages of at least three experiments and the standard deviations at any point do not exceed 5% of maximal (1.0).

decay is apparent for the D1-R64Q and the D1-R64E mutants. Numerical analysis of the decays, which could be adequately fit by assuming two exponentially decaying components, shows that Q_A^- decays are indeed decelerated in the D1-R64Q and the D1-R64E mutants (not shown). Since changes in the midpoint potential of the reactants of the $S_2Q_A^-$ state are expected to be revealed by the fluorescence measurements shown in Figure 4, the accelerated S-state decays shown in Figure 3 are probably not due to changes in the midpoint potential of the $(Mn)_4$ cluster. Rather, the changes in the S-state lifetimes are probably due to alterations in either the Q_B site or other reactants as discussed below.

Previous studies have demonstrated that the absence or defective binding of the extrinsic proteins causes the relatively facile loss of the active site metal ions and loss of O_2 evolution in vivo. The stability of O_2-evolving activity in whole cell samples incubated in the dark is shown in Figure 5. Both the D1-R64E and D1-R64Q displayed pronounced declines in O_2 evolution in comparison to the wild-type. Brief illumination of these samples restored activities to levels approaching (>90%) their original pre-incubation values. Photoreversible loss of O_2 evolution activity is associated with absence of MSP (*53*, *54*), absence of cytochrome c_{550} (*55*), and certain mutations in the e-loop of CP47 (*42*, *53*−*55*). Because of the similarities with the process of photoactivation, it has been assumed that the light-dependent restoration of O_2 evolution is due to the re-binding of Mn atoms lost during the dark incubation period.

Previous work has demonstrated an increase in the relative quantum yield of photoactivation in mutants that lack or have impaired binding of extrinsic proteins (*25*, *54*). Cells were extracted with hydroxylamine to extract the $(Mn)_4$ cluster and subjected to flash illumination to study the light-driven assembly of the $(Mn)_4$ cluster (photoactivation). As shown in Figure 6 all strains were capable of photoactivation under these conditions with the D1-R64E strain exhibiting the highest relative quantum yield of the group. Increases in the quantum yield of photoactivation have been hypothesized to reflect increased access of Mn^{2+} ions to the site of photoligation, although other possibilities such as an increased relative pool size of the electron acceptor are not

excluded. In related flash interval dependence photoactivation experiments (not shown), the D1-R64E mutant was shown to cause a pronounced decrease in the stability of the intermediates of the photoactivation reaction similar to the destabilization previously shown to be the result of mutations at the nearby D1-D59 and D1-D61 positions.

DISCUSSION

The directed mutations of the strictly conserved arginine at position 64 of the D1 protein, located in the lumenal a−b loop, have a significant deleterious effect upon the binding of MSP and, to a lesser extent, cytochrome c_{550} (Figure 1). Previous experiments analyzing different mutations in the lumenally exposed e-loop of CP47, using the same binding assay (*43*), located specific arginine residues involved in MSP binding in a region of the CP47 protein previously identified as an MSP binding domain by biochemical studies (*20*−*22*, *56*, *57*). Here we find that replacement of the basic arginine side chain with the glutamic acid side chain resulted in the most severe impact, whereas substitutions with glutamine and valine had less impact on binding. Decreases in the number of PSII centers estimated from variable fluorescence correlated well with oxygen evolution, except for D1-R64E, which had a larger decrease in O_2 evolution (Table 1). This suggests that the R64 mutations had an impact upon the cellular accumulation of PSII, which has been observed for other PSII mutations and is generally ascribed to decreased stability of the complex (*58*, *59*). For those PSII centers that do accumulate, the mutations cause functional changes in the H_2O-oxidase including changes in the O_2 release kinetics and stability of the S-states, that coincide with the weakened binding of the extrinsic proteins.

These findings are similar to those obtained from the analysis of mutations of the arginines 384 and 385 in the e-loop of CP47 (*39*). In that study, it was found that replacement of the arginines with oppositely charged glutamates greatly weakened the binding of MSP, whereas substitution with glycines resulted in a less drastic weakening of binding. Ionic interactions are proposed to play an important role in binding the extrinsic proteins to the lumenal portion of the PSII complex, with at least two studies finding carboxylate residues on MSP important for binding (*16*, *26*) (but see ref *23* for alternative view). It is therefore possible that D1-R64 forms a salt bridge with an oppositely charged acidic residue of an extrinsic protein. Alternatively, the D1-R64E mutation results in a less direct structural perturbation of the PSII complex that weakens the binding of the extrinsic proteins. The current PSII crystal structure model does not permit clarification of this point, especially since the interhelical lumenal domains, which are postulated to form these sites, are unresolved at this stage of the structural refinement (*1*). Nevertheless, MSP is assigned a position directly above the helices connected by the D1 a−b loop, and therefore the present results are consistent with, but obviously do not prove, a direct interaction between MSP and D1. Antibody studies have shown that epitopes on the D1 a−b lumenal loop were exposed upon removal of active site Mn as well as the extrinsic proteins by washing with Tris (*60*). MSP was observed to be chemically cross-linked to the D1 and D2 polypeptides (*61*), and the [D1/D2/cyt. b_{559}PsbI] reaction center complex has been affinity purified using immobilized MSP (*62*). We observed here that the binding of MSP and cytochrome c_{550} are both weakened, albeit to a lesser extent for cytochrome c_{550}, especially by the D1-R64E mutation. This result is qualitatively consistent with biochemical studies that demonstrated a weak augmentation of cytochrome c_{550} binding in the presence of bound MSP in *S. elongatus* (*19*), but in contrast to studies with the red alga *C. caldarium* (*19*). However, our results indicate greater loss of cytochrome c_{550} binding than would be expected from previous results (*19*). Furthermore, the observation that cytochrome c_{550} appears to be situated a considerable distance from the resolved portions of MSP in the crystal structure (*1*) and the finding that cytochrome c_{550} cross-links to the D2 protein (*34*) make a direct interaction between MSP and cytochrome c_{550} less likely as an explanation to account for the correlated weakening of binding of the two extrinsic proteins. Therefore, we conclude that mutation of R64 also produces an indirect structural rearrangement of the PSII core that probably affects the binding of both polypeptides.

Altered binding of the extrinsic proteins is also consistent with the finding that O_2 evolution activity rapidly decays in a photoreversible manner in the D1-R64E and D1-R64Q mutants. Dark deactivation of O_2 evolution is also observed in the ΔpsbO and ΔpsbV mutants lacking MSP and cytochrome c_{550}, respectively (*49*, *55*). This has been interpreted to reflect facile loss of Mn from the active site by analogy with biochemical depletion experiments testing the effects of MSP removal upon the stability of the (Mn_4). The reactivation of in vivo dark deactivated samples by light treatment has been interpreted to correspond to re-ligation of Mn^{2+} upon oxidation by the photochemical reaction center (Figure 5). It is interesting to compare the present results with those obtained with the CP47-RR384385EE mutants (*25*, *43*) and CP47 mutants containing short deletions in the e-loop (*42*, *63*). Both the D1-R64E and the CP47-RR384385EE exhibit similar decreases in the binding affinity for MSP and both show slow downs of the O_2 release kinetics during the S_3-[S_4]-S_0 transition. However, unlike the D1-R64E mutant, the CP47-RR384385EE did not exhibit a pronounced tendency to deactivate in the dark. The fact that the D1-R64E is dark unstable, whereas the CP47-RR384385EE mutant is not, suggests that these different mutations affect separate points of interaction between MSP and the intrinsic portion of the reaction center core complex. However, several mutants having short deletions in the e-loop of CP47 also result in a greatly decreased binding affinity of MSP and a dark instability of the $(Mn)_4$ (*42*, *63*). This would be consistent with numerous observations suggesting that MSP contacts multiple subunits of the integral PSII complex (reviewed in ref *64*). At the same time, it is important to note that our present observations are consistent with the possibility that the R64 mutations exert a more generalized disruptive effect upon the conformation of PSII impacting MSP binding. Unlike the disruption of MSP binding in the CP47-RR384385EE mutant, corroboration of a specific protein−protein contact by chemical cross-linking experiments has not yet been demonstrated.

The D1 a−b loop has been proposed to be part of a Ca^{2+} binding site on the basis of sequence analysis and growth characteristics of strains having mutations in this region. As with the D1-D59 and D1-D61 mutants, the D1-R64E and D1-R64Q mutations increased the demand for Ca^{2+} in the

growth medium during autotrophic growth. If the D1-D59 and D1-D61 form the initial two aspartates of a characteristic Ca^{2+}-binding sequence motif, -D−X−D−X, as previously proposed (*46*, *65*), then an arginine at 64 would occupy a less stringently maintained position according to sequence comparisons. While it is improbable that the guanidinium group of the arginine side chain ligands to Ca^{2+}, there is precedence in known Ca^{2+}-binding structures [e.g., myosin light chain (*66*)] wherein the backbone portion of the arginine only weakly interacts with the calcium ion and the side-chain is oriented away from the coordination sphere. In those cases, the basic residue may form half of a salt-bridge that stabilizes an interaction between the Ca^{2+} binding loop and another domain or subunit of the protein. However, the increased Ca^{2+} requirement by the R64 mutants is a characteristic shared by a variety of other apparently disparate mutations of the PSII complex. These include: (i) deletion of MSP, (ii) deletion of cytochrome c_{550}, (iii) mutations in the CP47 protein affecting MSP binding, and (iv) mutations of the carboxy terminus of the D1 protein. Assuming the Ca^{2+}-sensitive growth phenotype is due to a single cause, these different mutations would appear to affect a common process or structural feature. For example, if high local concentrations of Ca^{2+} are necessary for maximal oxidase activity, possibly the various mutations alter the structure allowing for ready loss of Ca^{2+}.

A common feature of all the above-mentioned mutants is an absence or alteration in the binding of the extrinsic proteins. In the case of the D1 carboxy terminal mutants, an alteration in the binding of MSP has been deduced on the basis of an increased accessibility of endogenous Mn to the high affinity Mn-binding site (*45*). Accordingly, there appears to be correlation in the binding of the extrinsic proteins and the ability to grow autotrophically at diminished calcium concentrations. As with the extrinsic protein binding sites, the current structural resolution has not yet allowed placement of the PSII Ca^{2+}. While the location of Ca^{2+} is not resolved in the cyanobacterial PSII crystal structure, a cadmium ion used to provide isomorphic replacement information is situated in the crystal structure in the lumenal domain at a location between MSP and the a and b helices of the D1 protein (*1*). Since, Cd^{2+} is known to substitute for Ca^{2+} in a variety of Ca^{2+}-binding proteins and specifically competes with Ca^{2+} at its PSII binding site with the loss of H_2O-oxidation activity upon replacement (*67*), the crystallographically located Cd^{2+} conceivably is occupying the enzymatically important Ca^{2+}-binding site. On the other hand, the several lines of evidence favor a very close proximity between the functional Ca^{2+} binding site and the $(Mn)_4$, which would exclude the crystallographically located Cd^{2+} as occupying the functional Ca^{2+} site since the Cd^{2+} and $(Mn)_4$ sites are approximately 29 Å apart in the crystal structure. Furthermore, replacement of Ca^{2+} with Cd^{2+} has been done using higher plant PSII membranes that were salt-washed to remove the 18- and 23-kDa proteins, and the 23-kDa protein seems help the retention of Ca^{2+} that would otherwise be lost during S-state turnover (*68*). These observations are difficult to reconcile with the crystallographically located Cd^{2+} as occupying the functional Ca^{2+} site since the 23-kDa protein would appear to be located on the opposite side of the PSII complex if it occupies the position corresponding to cytochrome c_{550}.

Mutations at position R64 had only a minor effect upon the back-reaction of the S_2-Q_A^- state as monitored by the fluorescence decay in the presence of DCMU. Since Q_A^- is thought to recombine with the S_2 state via $P680^+$, the rate of charge recombination via this pathway, the fluorescence decay rate reflects the quasi-equilibrium concentration of $P680^+$ present due to the reaction $S_2P680 \leftrightarrow S_1P680^+$. Changes in the midpoint potential of the S-system and/or P680 are expected to affect this equilibrium, and therefore if such changes exist, then the rate of fluorescence decay should be altered. Since the changes in the decay of fluorescence are small, then we conclude that the R64 mutations do not significantly affect the $S_2P680 \leftrightarrow S_1P680^+$ equilibrium and, hence, probably do not affect the redox potentials of either of these reactants. On the other hand, the decay of the S_2 and S_3 states was found to be considerably accelerated in the D1-R64E mutant and slightly accelerated in the D1-R64Q mutant. Consequently, accelerated S-state decays shown in Figure 3 are probably due to something other than a change in the midpoints of the redox active groups within the WOC. This situation contrasts with the previously measured D1 a−b loop mutants at position aspartate 59 and aspartate 61. These mutants were previously shown to exhibit accelerations of both fluorescence decay in the presence of DCMU (*46*) and S-state decay (*37*) as measured using the double flash technique employed in the present study.

At least two alternatives can be considered to account for accelerated S-state decays in the absence of changes in the $S_2P680 \leftrightarrow S_1P680^+$ equilibrium. The first alternative is that the mutation affects the Q_B site despite the fact that it is likely situated on the opposite of the membrane. If the redox potential of the Q_B/Q_B^- is shifted to more negative values, then the redox equilibrium between the Q_A and Q_B site would be shifted such that an electron at the Q_B site would be less deeply trapped thereby increasing the probability of back-reaction of the electron from Q_B^- to Q_A. The back-reaction of Q_A^- to the S_2 state of the WOC is fast (e.g., Figure 4) as compared to this de-trapping of the electron from Q_B^- and is likely to be the rate-limiting step for S-state decays which have half times in the tens of seconds. This back-reaction would be the rate-limiting step for S-state decays which have half times in the tens of seconds, since the half-time of back-reaction whereby Q_A^- reduces S_2 to S_1 is roughly a second as estimated by fluorescence decay in the presence of DCMU (e.g., Figure 4). A prediction of this alternative is that in the rate of forward electron transfer from Q_A^- to plastoquinol at the Q_B site would be retarded due to the hypothesized downshift in the midpoint of Q_B/Q_B^-. However, this does not seem to be the case since fluorescence decay in the absence of DCMU is not affected in the mutant (data not shown). A second alternative is that the accelerated deactivation of the S-states occurs via a pathway not involving Q_A. Since reduced Y_D of the D2 protein is thought to contribute to the deactivation of the S-states, enhancement of this avenue of WOC reduction is a candidate for the increased rate of dark deactivation of the higher S-states. Consistent with this possibility is the fact that kinetic analysis shows that the increased deactivation rate is largely due to an increase in the fast phase of deactivation (not shown), which is thought to be due to this pathway. We tentatively conclude, therefore, that the mutations at R64 affect either the relative

concentration of the reduced form of Y_D or that its intrinsic reactivity is increased by the mutations. However, we cannot exclude other alternatives. For example, Q_B^-, could be more rapidly oxidized by the S_2 and S_3 states of the WOC via an alternative pathway not involving Q_A that becomes thermodynamically more favorable or kinetically more accessible as a consequence of the mutations at R64. This might happen if the rate of the hypothesized cyclic PSII pathway involving cytochrome b_{559} (*69*−*72*) and perhaps carotenoid (*73*) is increased.

ACKNOWLEDGMENT

The authors thank Dr. Antony Crofts for useful discussions regarding S-state decay pathways and Dr J-R. Shen for insights and observations regarding extrinsic protein binding.

REFERENCES

1. Zouni, A., Witt, H. T., Kern, J., Fromme, P., Krauss, N., Saenger, W., and Orth, P. (2001) *Nature 409*, 739−43.
2. Bricker, T. M., and Ghanotakis, D. F. (1996) in *Oxygenic Photosynthesis: The Light Reactions* (Ort, D., and Yocum, C. F., Eds.) pp 113−136, Kluwer Academic Publishers, Dordrect, The Netherlands.
3. Britt, R. D. (1996) in *Oxygenic Photosynthesis: The Light Reactions* (Ort, D., and Yocum, C. F., Eds.) pp 137−164, Kluwer Academic Publishers, Dordrect, The Netherlands.
4. Diner, B. A., and Babcock, G. T. (1996) in *Oxygenic Photosynthesis: The Light Reactions* (Ort, D., and Yocum, C. F., Eds.) pp 213−247, Kluwer Academic Publishers, Dordrect, The Netherlands.
5. Debus, R. J. (2000) in *Metal Ions in Biological Systems* (Sigel, A., and Sigel, H., Eds.) pp 657−711, Marcel Dekker, New York.
6. Hoganson, C., Lydakis-Simantiris, N., Tang, X., Tommos, C., Warnke, K., Babcock, G., Diner, B., McCraken, J., and Styring, S. (1995) *Photosynth. Res. 46*, 177−184.
7. Szalai, V. A., Kuhne, H., Lakshmi, K. V., and Brudvig, G. W. (1998) *Biochemistry 37*, 13594−603.
8. Westphal, K. L., Tommos, C., Cukier, R. I., and Babcock, G. T. (2000) *Curr. Opin. Plant Biol. 3*, 236−42.
9. Tommos, C., and Babcock, G. T. (2000) *Biochim. Biophys. Acta 1458*, 199−219.
10. Boekema, E. J., Nield, J., Hankamer, B., and Barber, J. (1998) *Eur. J. Biochem. 252*, 268−76.
11. Hankamer, B., Morris, E. P., and Barber, J. (1999) *Nat. Struct. Biol. 6*, 560−564.
12. Kuhl, H., Rogner, M., Van Breemen, J. F., and Boekema, E. J. (1999) *Eur. J. Biochem. 266*, 453−459.
13. Kuhl, H., Kruip, J., Seidler, A., Krieger-Liszkay, A., Bunker, M., Bald, D., Scheidig, A. J., and Rogner, M. (2000) *J. Biol. Chem. 275*, 20652−9.
14. Nield, J., Orlova, E. V., Morris, E. P., Gowen, B., van Heel, M., and Barber, J. (2000) *Nat. Struct. Biol. 7*, 44−7.
15. Shen, J. R., and Kamiya, N. (2000) *Biochemistry 39*, 14739−44.
16. Seidler, A. (1996) *Eur. J. Biochem. 242*, 485−490.
17. Navarro, J. A., Hervas, M., De la Cerda, B., and De la Rosa, M. A. (1995) *Arch. Biochem. Biophys. 3186*, 46−52.
18. Frazao, C., Enguita, F. J., Coelho, R., Sheldrick, G. M., Navarro, J. A., Hervas, M., De la Rosa, M. A., and Carrondo, M. A. (2001) *J. Biol. Inorg. Chem. 6*, 324−32.
19. Enami, I., Kikuchi, S., Fukuda, T., Ohta, H., and Shen, J. R. (1998) *Biochemistry 37*, 2787−93.
20. Odom, W., and Bricker, T. M. (1992) *Biochemistry 31*, 5616−5620.
21. Frankel, L. K., and Bricker, T. M. (1992) *Biochemistry 31*, 11059−11064.
22. Frankel, L. K., and Bricker, T. M. (1995) *Biochemistry 34*, 7492−7497.
23. Miura, T., Shen, J. R., Takahashi, S., Kamo, M., Nakamura, E., Ohta, H., Kamei, A., Inoue, Y., Domae, N., Takio, K., Nakazato, K., and Enami, I. (1997) *J. Biol. Chem. 272*, 3788−3798.
24. Haag, E., Eaton-Rye, J. J., Renger, G., and Vermaas, W. F. J. (1993) *Biochemistry 32*, 4444−4454.
25. Putnam-Evans, C., Burnap, R., Wu, J., Whitmarsh, J., and Bricker, T. M. (1996) *Biochemistry 35*, 4046−4053.
26. Frankel, L. K., Cruz, J. A., and Bricker, T. M. (1999) *Biochemistry 38*, 14271−8.
27. Isogai, Y., Itoh, S., and Nishimura, M. B. B. A. (1990) *Biochim. Biophys. Acta 1017*, 204−208.
28. Andersson, B., Larsson, C., Jansson, C., Ljungberg, U., and Akerland, H.-E. (1984) *Biochim. Biophys. Acta 766*.
29. Miyao, M., and Murata, N. (1989) *Biochim. Biophys. Acta 977*, 315−321.
30. Kavelaki, K., and Ghanotakis, D. F. (1991) *Photosynth. Res. 29*, 149−155.
31. Bernier, M., and Carpentier, R. (1995) *FEBS Lett. 360*, 251−4.
32. de Vitry, C., Olive, J., Drapier, D., Recouvreur, M., and Wollman, F. A. (1989) *J. Cell Biol. 109*, 991−1006.
33. Shen, J.-R., and Inoue, Y. (1993) *Biochemistry 32*, 1825−1832.
34. Han, K. C., Shen, J. R., Ikeuchi, M., and Inoue, Y. (1994) *FEBS Lett. 355*, 121−124.
35. Shen, J. R., Burnap, R. L., and Inoue, Y. (1995) *Biochemistry 34*, 12661−12668.
36. Hundelt, M., Hays, A. M., Debus, R. J., and Junge, W. (1998) *Biochemistry 37*, 14450−6.
37. Qian, M., Dao, L., Debus, R. J., and Burnap, R. L. (1999) *Biochemistry 38*, 6070−6081.
38. Williams, J. G. K. (1988) *Methods Enzymol. 167*, 766−778.
39. Boerner, R. J., Nguyen, A. P., Barry, B. A., and Debus, R. J. (1992) *Biochemistry 31*, 6660−6672.
40. Burnap, R., Koike, H., Sotiropoulou, G., and Sherman, L. A., Inoue, Y. (1989) *Photosynth. Res. 22*, 123−130.
41. Burnap, R. L., Qian, M., Shen, J. R., Inoue, Y., and Sherman, L. A. (1994) *Biochemistry 3307*, 13712−13718.
42. Gleiter, H. M., Haag, E., Shen, J. R., Eaton Rye, J. J., Inoue, Y., Vermaas, W. F., and Renger, G. (1994) *Biochemistry 33*, 12063−12071.
43. Qian, M., Al Khaldi, S. F., Putnam Evans, C., Bricker, T. M., and Burnap, R. L. (1997) *Biochemistry 36*, 15244 52.
44. Shen, J. R., Vermaas, W., and Inoue, Y. (1995) *J. Biol. Chem. 270*, 6901 6907.
45. Chu, H.-A., Nguyen, A. P., and Debus, R. A. (1994) *Biochemistry 33*, 6150−6157.
46. Chu, H. A., Nguyen, A. P., and Debus, R. J. (1995) *Biochemistry 34*, 5839−5858.
47. Nixon, P. J., and Diner, B. A. (1992) *Biochemistry 31*, 942 8.
48. Cheniae, G. M., and Martin, I. F. (1972) *Plant Physiol. 50*, 87−94.
49. Burnap, R. L., Qian, M., Al-Khaldi, S., and Pierce, C. (1995) in *Photosynthesis: From Light to Biosphere* (Mathis, P., Ed.), Kluwer Academic Publishers, Dordrect, The Netherlands.
50. Lichtenthaler, H. K. (1987) *Methods Enzymol. 148*, 350−382.
51. Chu, H.-A., Nguyen, A. P., and Debus, R. A. (1994) *Biochemistry 33*, 6137−6149.
52. Philbrick, J. B., Diner, B. A., and Zilinskas, B. A. (1991) *J. Biol. Chem. 266*, 13370−13376.
53. Engels, D. H., Lott, A., Schmid, G. H., and Pistorious, E. K. (1994) *Photosynth. Res. 42*, 227−244.
54. Burnap, R. L., Qian, M., and Pierce, C. (1996) *Biochemistry 35*, 874−882.
55. Shen, J. R., Qian, M., Inoue, Y., and Burnap, R. L. (1998) *Biochemistry 37*, 1551−8.
56. Bricker, T. M., Odom, W. R., and Queirolo, C. B. (1988) *FEBS Lett. 231*, 111−117.
57. Hayashi, H., Fujimura, Y., Mohanty, P., and Murata, N. (1993) *Photosynth. Res. 36*, 35−42.
58. Vermaas, W. F. J., Ikeuchi, M., and Inoue, Y. (1988) *Photosynth. Res. 17*, 97−114.

59. Salih, G., Wiklund, R., Tyystjarvi, T., Maenpaa, P., Gerez, C., and Jansson, C. (1996) *Photosynth. Res. 49*, 131−140.
60. Sayre, R. T., Andersson, B., and Bogorad, L. (1986) *Cell 47*, 601−8.
61. Mei, R., Green, J. P., Sayre, R. T., and Frasch, W. D. (1989) *Biochemistry 28*, 5560−7.
62. Gounaris, K., Chapman, D. J., and Barber, J. (1988) *Fed. Eur. Biochem. Soc. Lett. 234*, 374−378.
63. Gleiter, H. M., Haag, E., Shen, J. R., Eaton Rye, J. J., Seeliger, A. G., Inoue, Y., Vermaas, W. F., and Renger, G. (1995) *Biochemistry 34*, 6847−6856.
64. Seidler, A., and Rutherford, A. W. (1996) *Biochemistry 35*, 12104 10.
65. Dismukes, G. C. (1988) *Chem. Scr. 28A*, 99−104.
66. Houdusse, A., Kalabokis, V. N., Himmel, D., Szent-Gyorgyi, A. G., and Cohen, C. (1999) *Cell 97*, 459−70.
67. Matysik, J., Alia, A., Nachtegaal, G., van Gorkom, H. J., Hoff, A. J., and de Groot, H. J. (2000) *Biochemistry 39*, 6751−5.
68. Adelroth, P., Lindberg, K., and Andreasson, L. E. (1995) *Biochemistry 34*, 9021 9027.
69. Falkowski, P. G., Fujita, Y., Ley, A., and Mauzerall, D. (1986) *Plant Physiol. 81*, 310−312.
70. Thompson, L. K., and Brudvig, G. W. (1988) *Biochemistry 27*, 6653−6658.
71. Poulson, M., Samson, G., and Whitmarsh, J. (1995) *Biochemistry 34*, 10932−10938.
72. Prasil, O., Kolber, Z., Berry, J. A., and Falkowski, P. G. (1996) *Photosynth. Res. 48*, 395−410.
73. Hanley, J., Deligiannakis, Y., Pascal, A., Faller, P., and Rutherford, A. W. (1999) *Biochemistry 38*, 8189−95.
74. Lavorel, J. (1976) *J. Theor. Biol. 57*, 171−185.
75. Meunier, P. C., Burnap, R. L., and Sherman, L. A. (1995) *Photosynth. Res. 47*, 61−76.
76. Jursinic, P. A., and Dennenberg, R. J. (1990) *Biochim. Biophys. Acta 1020*, 195−206.
77. Forbush, B., Kok, B., and McGloin, M. P. (1971) *Photochem. Photobiol. 14*, 307−321.
78. Seeliger, A. G., Kurreck, J., and Renger, G. (1997) *Biochemistry 36*, 2459 64.

BI0100135